

Diphoton rate in the Inert Doublet Model with a 125 GeV Higgs boson

Bogumiła Świeżewska, Maria Krawczyk

*Faculty of Physics, University of Warsaw
Hoża 69, 00-681 Warsaw, Poland*

May 10, 2022

Abstract

We performed an analysis of the diphoton decay rate of the Higgs boson in the Inert Doublet Model. We found conditions necessary for the enhancement in that channel in terms of constraints on masses of the charged scalar and the Dark Matter particle.

1 Introduction

Recently a Higgs-like boson has been discovered at the Large Hadron Collider (LHC) [1,2]. Although most of the measurements of its properties are in agreement with the hypothesis of the Standard Model (SM) Higgs particle, there may be some indications that the discovered boson is not fully SM-like. Among these is the signal strength in the decay channel $h \rightarrow \gamma\gamma$, $R_{\gamma\gamma}$, which is proportional to $\text{Br}(h \rightarrow \gamma\gamma)$. According to the latest experimental results [3] $R_{\gamma\gamma} = 1.8 \pm 0.3$. This can be accounted for in the framework of Two Higgs Doublet Models (2HDM), in particular in the Inert Doublet Model (IDM).

The diphoton decay rate was considered in Ref. [4–7]. In the parameter region studied in Ref. [4] no enhancement was found, while in Ref. [5] the possibility of modifying the total decay width of the Higgs boson due to the invisible decays into Dark Matter (DM) was not taken into account. In Ref. [6] not entire parameter space was investigated as the mass parameter of the potential was taken with only one sign, the DM particle was assumed to be lighter than the Higgs boson and the mass of DM was strongly constrained ($M_H < 150$ GeV). Analysis [7] followed the approach of Ref. [6].

We present an independent analysis of the diphoton Higgs decay mode which improves the points mentioned above and makes use of the recent experimental data [1,2]. The paper is organized as follows: in Section 2 we briefly review the model, describe the constraints taken into account and present the method of the analysis. In Section 3 possible sources of modifications of the diphoton production rate in the IDM with respect to the SM are discussed. The results are presented in Section 4 and a short summary can be found in Section 5.

2 Setup of the analysis

2.1 Model

We consider the IDM [4, 8, 9], which is a 2HDM with the following potential for two SU(2) doublets ϕ_S , ϕ_D with hypercharge $Y = 1$,

$$V = -\frac{1}{2} \left[m_{11}^2 (\phi_S^\dagger \phi_S) + m_{22}^2 (\phi_D^\dagger \phi_D) \right] + \frac{1}{2} \left[\lambda_1 (\phi_S^\dagger \phi_S)^2 + \lambda_2 (\phi_D^\dagger \phi_D)^2 \right] + \lambda_3 (\phi_S^\dagger \phi_S) (\phi_D^\dagger \phi_D) + \lambda_4 (\phi_S^\dagger \phi_D) (\phi_D^\dagger \phi_S) + \frac{1}{2} \lambda_5 \left[(\phi_S^\dagger \phi_D)^2 + (\phi_D^\dagger \phi_S)^2 \right]. \quad (1)$$

The parameters m_{11}^2 , m_{22}^2 and $\lambda_1 \dots \lambda_4$ are real numbers and without loss of generality we take $\lambda_5 < 0$ [10–12]. The potential V is invariant under a \mathbb{Z}_2 type symmetry, called D , which changes the sign of the ϕ_D doublet and leaves all other fields unchanged.

We consider a D -symmetric vacuum state (Inert vacuum), which corresponds to $\langle \phi_S \rangle = \begin{pmatrix} 0 \\ v/\sqrt{2} \end{pmatrix}$, $\langle \phi_D \rangle = 0$. The masses of the physical scalars read:

$$\begin{aligned} M_h^2 &= m_{11}^2 = \lambda_1 v^2, \\ M_{H^\pm}^2 &= \frac{1}{2} (\lambda_3 v^2 - m_{22}^2), \\ M_A^2 &= \frac{1}{2} (\lambda_{345} v^2 - m_{22}^2) = M_{H^\pm}^2 + \frac{1}{2} \lambda_{45}^- v^2, \\ M_H^2 &= \frac{1}{2} (\lambda_{345} v^2 - m_{22}^2) = M_{H^\pm}^2 + \frac{1}{2} \lambda_{45} v^2, \end{aligned}$$

where $\lambda_{345} = \lambda_3 + \lambda_4 + \lambda_5$, $\lambda_{345}^- = \lambda_3 + \lambda_4 - \lambda_5$, $\lambda_{45}^- = \lambda_4 - \lambda_5$, $\lambda_{45} = \lambda_4 + \lambda_5$. The parameters λ_3 and λ_{345} are important for our analysis as they represent the hH^+H^- and hHH couplings, respectively.

Only the ϕ_S doublet takes part in the Spontaneous Symmetry Breaking (SSB) so only h is a Higgs boson. The remaining scalars are often called inert scalars¹ as they do not contribute to SSB.

We assume the Yukawa interactions of Type I, so only the ϕ_S doublet couples to fermions. Thus h is SM-like, i.e. it couples to fermions (at the tree-level) just like the SM Higgs and so does to the gauge bosons. We assume that it corresponds to the boson discovered at the LHC in 2012 [1, 2] and set $M_h = 125$ GeV.

Since the D symmetry is exact in the IDM, it renders the lightest neutral D -odd particle stable providing a good Dark Matter (DM) candidate. We will assume that the DM particle is the H scalar, so $\lambda_{45} < 0$. By definition the DM particle is the lightest of the D -odd scalars, not of all scalars, as assumed in Ref. [6].

2.2 Constraints

In our analysis we take into account the following constraints [13]:

Vacuum stability For a stable vacuum state to exist it is necessary that the potential V is bounded from below, this leads to [8]:

$$\lambda_1 > 0, \quad \lambda_2 > 0, \quad \lambda_3 + \sqrt{\lambda_1 \lambda_2} > 0, \quad \lambda_{345} + \sqrt{\lambda_1 \lambda_2} > 0,$$

Perturbative unitarity For the theory to be perturbatively unitary it is required that the eigenvalues Λ_i of the high-energy scattering matrix fulfill the condition $|\Lambda_i| < 8\pi$, [13–15].

Existence of the Inert vacuum The Inert vacuum can be realized only if the following conditions are fulfilled [10, 16]:

$$M_h^2, M_H^2, M_A^2, M_{H^\pm}^2 \geq 0, \quad \frac{m_{11}^2}{\sqrt{\lambda_1}} > \frac{m_{22}^2}{\sqrt{\lambda_2}}.$$

From the existence of the Inert vacuum and unitarity bounds on λ_2 , for $M_h = 125$ GeV, follows a bound on m_{22}^2 [13]:

$$m_{22}^2 \lesssim 9 \cdot 10^4 \text{ GeV}^2. \quad (2)$$

H as DM candidate We assume that H is the DM candidate, so $M_H < M_A, M_{H^\pm}$. Studies of the DM in the IDM [17–20] show that if H is to account for the observed energy relic density of DM, it should have mass in one of the three regions: $M_H < 10$ GeV, $40 \text{ GeV} < M_H < 80 \text{ GeV}$ or $M_H > 500 \text{ GeV}$. We will not impose these bounds from the very beginning, but we will discuss the consistency of our results with these constraints.

Electroweak Precision Tests (EWPT) We demand that the values of S and T parameters calculated in the IDM (using formulas from [9]) lie within 2σ ellipses in the S, T plane, with the following central values [21]: $S = 0.03 \pm 0.09$, $T = 0.07 \pm 0.08$. The correlation of the fit is equal to 87%.

LEP We use the LEPI and LEPII bounds on the scalar masses [22, 23]:

$$M_{H^\pm} + M_H > M_W, \quad M_{H^\pm} + M_A > M_W, \quad M_H + M_A > M_Z, \quad 2M_{H^\pm} > M_Z, \quad M_{H^\pm} > 70 \text{ GeV},$$

and exclude the region where: $M_H < 80 \text{ GeV}$ and $M_A < 100 \text{ GeV}$ and $M_A - M_H > 8 \text{ GeV}$.

We will refer to the set of the conditions described above as “the constraints” for simplicity.

2.3 Method of the analysis

We scanned randomly the parameter space of the IDM, taking into account the constraints and letting the parameters to vary in the following regimes:

$$\begin{aligned} M_h &= 125 \text{ GeV}, \\ 70 \text{ GeV} &\leq M_{H^\pm} \leq 800 \text{ GeV} (1400 \text{ GeV}), \\ 0 &< M_A \leq 800 \text{ GeV} (1400 \text{ GeV}), \\ 0 &< M_H < M_A, M_{H^\pm}, \\ -25 \cdot 10^4 \text{ GeV}^2 &(-2 \cdot 10^6 \text{ GeV}^2) \leq m_{22}^2 \leq 9 \cdot 10^4 \text{ GeV}^2, \\ 0 &< \lambda_2 \leq 10. \end{aligned}$$

The allowed region in the parameter space depends on the choice of minimal value of m_{22}^2 , which is not constrained. We considered two regimes for m_{22}^2 , narrow and wide, for which larger masses of dark scalars are allowed, up to 1400 GeV (values in brackets).

In addition we checked which of the points in the parameter space fulfill the condition $R_{\gamma\gamma} > 1$.

¹They are also called dark scalars (D -scalars).

3 $R_{\gamma\gamma}$

We define the quantity $R_{\gamma\gamma}$ as follows [6]:

$$R_{\gamma\gamma} := \frac{\sigma(pp \rightarrow h \rightarrow \gamma\gamma)^{\text{IDM}}}{\sigma(pp \rightarrow h \rightarrow \gamma\gamma)^{\text{SM}}} = \frac{(\sigma(gg \rightarrow h)\text{Br}(h \rightarrow \gamma\gamma))^{\text{IDM}}}{(\sigma(gg \rightarrow h)\text{Br}(h \rightarrow \gamma\gamma))^{\text{SM}}} = \frac{\text{Br}(h \rightarrow \gamma\gamma)^{\text{IDM}}}{\text{Br}(h \rightarrow \gamma\gamma)^{\text{SM}}}.$$

Above we used the fact that the gluon fusion is the dominant channel of Higgs production. Moreover, in the IDM $\sigma(gg \rightarrow h)^{\text{IDM}} = \sigma(gg \rightarrow h)^{\text{SM}}$, so $R_{\gamma\gamma}$ reduces to the ratio of branching ratios.

In the IDM this ratio can be modified with respect to the SM, since the charged scalar exchanged in loops gives extra contribution to the $h \rightarrow \gamma\gamma$ amplitude [4–6]. In addition, the total decay width of the Higgs boson can be modified due to existence of invisible decay channels $h \rightarrow HH$ and $h \rightarrow AA$ [4, 6]. In different ranges of parameters, different effects dominate.

Many channels contribute to the total decay width of the Higgs boson h , the most important ones are: $b\bar{b}$, $c\bar{c}$, $\tau^+\tau^-$, ZZ^* , WW^* , $\gamma\gamma$, $Z\gamma$, gg , HH , AA . To compute the decay widths we used the formulas from Refs. [24–27]. For completeness they are summarized in the Appendix B. The partial widths of h decays into SM particles are as in the SM.

In Fig. 1 the h branching ratios of these channels are presented as a function of m_{22}^2 . Three different cases are considered: decay channels $h \rightarrow AA$ and $h \rightarrow HH$ are open (with $M_H = 50$ GeV, $M_A = 60$ GeV, left panel), $h \rightarrow AA$ is closed and $h \rightarrow HH$ is open ($M_A > 63$ GeV, $M_H = 60$ GeV, middle panel), both $h \rightarrow AA$ and $h \rightarrow HH$ are closed ($M_H = 75$ GeV, $M_A > 63$ GeV, right panel).

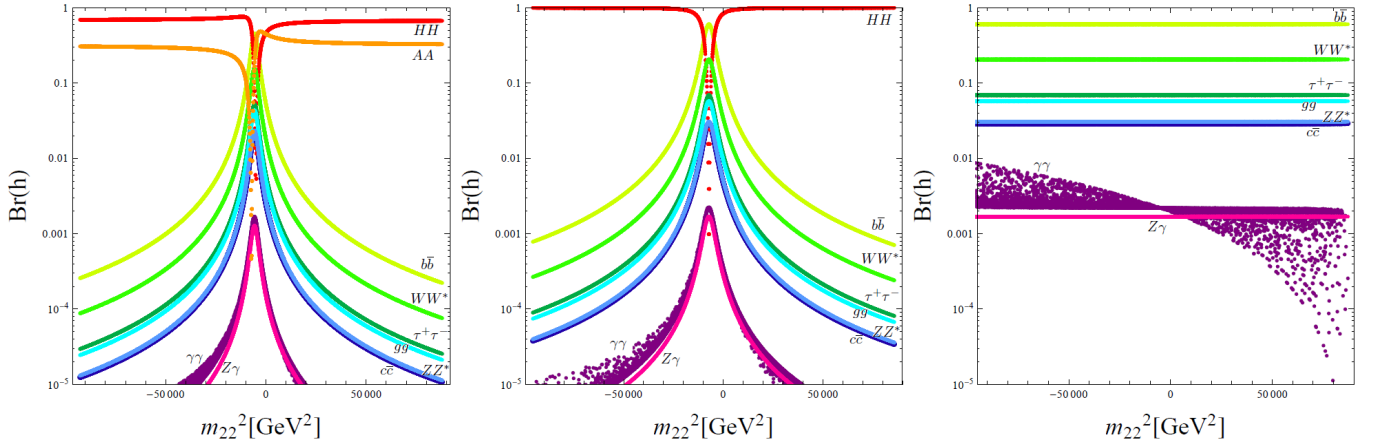


Figure 1: Branching ratios of Higgs boson decays. Left panel: decay channels $h \rightarrow HH$ and $h \rightarrow AA$ are open ($M_H = 50$ GeV, $M_A = 60$ GeV), middle panel: $h \rightarrow HH$ open ($M_H = 60$ GeV, $M_A > 63$ GeV), right panel: no invisible h decay channels allowed ($M_H = 75$ GeV, $M_A > 63$ GeV).

It appears, that when invisible decay channels $h \rightarrow HH$ and $h \rightarrow AA$ are open ($M_H < M_h/2$, $M_A < M_h/2$), their partial widths $\Gamma(h \rightarrow HH)$, $\Gamma(h \rightarrow AA)$ are big as compared to the partial widths of decays into SM particles. It will be shown, that in these cases the total decay width of the Higgs boson is so big that enhancing $\text{Br}(h \rightarrow \gamma\gamma)$ is impossible.

If the invisible decay channels are closed, all the branching ratios, except for the $\gamma\gamma$ channel, are constant. $\text{Br}(h \rightarrow \gamma\gamma)$ varies significantly with m_{22}^2 . We will analyze this case below.

3.1 $M_H > M_h/2$

When $M_H > M_h/2$ (and also $M_A > M_h/2$) the decay channels $h \rightarrow HH$ and $h \rightarrow AA$ are kinematically closed. Then, the total width of h is barely modified with respect to the SM case, since the branching ratio of $h \rightarrow \gamma\gamma$, which is the only process that receives contributions from dark scalars, is of order 10^{-4} . Thus $R_{\gamma\gamma}$ reduces to the ratio of the partial width in the IDM over the one in the SM.

$$\tilde{R}_{\gamma\gamma} = \frac{\Gamma(h \rightarrow \gamma\gamma)^{\text{IDM}}}{\Gamma(h \rightarrow \gamma\gamma)^{\text{SM}}}.$$

The partial width is given by [24, 25]:

$$\Gamma(h \rightarrow \gamma\gamma)^{\text{IDM}} = \frac{G_F \alpha^2 M_h^3}{128 \sqrt{2} \pi^3} \left| \underbrace{\frac{4}{3} A_{1/2} \left(\frac{4M_t^2}{M_h^2} \right) + A_1 \left(\frac{4M_W^2}{M_h^2} \right)}_{\mathcal{M}^{\text{SM}}} + \underbrace{\frac{2M_{H^\pm}^2 + m_{22}^2}{2M_{H^\pm}^2} A_0 \left(\frac{4M_{H^\pm}^2}{M_h^2} \right)}_{\delta \mathcal{M}^{\text{IDM}}} \right|^2,$$

where \mathcal{M}^{SM} denotes the contribution from the SM and $\delta\mathcal{M}^{\text{IDM}}$ is the extra contribution present in the IDM, $\mathcal{M}^{\text{IDM}} = \mathcal{M}^{\text{SM}} + \delta\mathcal{M}^{\text{IDM}}$. The form factors are defined as follows [28]:

$$\begin{aligned} A_0(\tau) &= -\tau[1 - \tau f(\tau)], \\ A_{1/2}(\tau) &= 2\tau[1 + (1 - \tau)f(\tau)], \\ A_1(\tau) &= -[2 + 3\tau + 3\tau(2 - \tau)f(\tau)] \end{aligned}$$

and

$$f(\tau) = \begin{cases} \arcsin^2\left(\frac{1}{\sqrt{\tau}}\right) & \text{for } \tau \geq 1, \\ -\frac{1}{4} \left[\log\left(\frac{1+\sqrt{1-\frac{1}{\tau}}}{1-\sqrt{1-\frac{1}{\tau}}}\right) - i\pi \right]^2 & \text{for } \tau < 1. \end{cases}$$

Above we do not include the contributions from the bottom and charm quark loops as well as from the τ loop, as we have checked that they are negligible. We take $M_W = 80.399 \text{ GeV}$ and $M_t = 173 \text{ GeV}$ from the Particle Data Group (PDG) analysis [27].

We consider the inequality $\tilde{R}_{\gamma\gamma} > 1$, which can be written as:

$$|\mathcal{M}^{\text{SM}} + \delta\mathcal{M}^{\text{IDM}}|^2 > |\mathcal{M}^{\text{SM}}|^2 \quad (3)$$

\mathcal{M}^{SM} is fixed² and $f\left(\frac{4M_{H^\pm}^2}{M_h^2}\right) = \arcsin^2\left(\frac{M_h}{2M_{H^\pm}}\right)$, because $M_H > M_h/2$. Inequality (3) can be solved analytically (the full derivation is given in Appendix A), giving the result that $R_{\gamma\gamma} > 1$ is possible only when:

$$m_{22}^2 < -2M_{H^\pm}^2 \quad \text{or} \quad m_{22}^2 > \frac{aM_h^2}{1 - \left(\frac{2M_{H^\pm}}{M_h}\right)^2 \arcsin^2\left(\frac{M_h}{2M_{H^\pm}}\right)} - 2M_{H^\pm}^2, \quad (4)$$

where $a = \text{Re}\mathcal{M}^{\text{SM}}$. This two conditions correspond to two possible cases: when the contribution of the charged scalar loop interferes constructively or destructively with the SM contributions. In the latter case the contribution from the charged scalar has to be at least twice as big as the SM term [5]. Since the functions in Eq. (4) are both monotonic we can get overall bounds on m_{22}^2 with use of the LEP II bound on mass of the charged scalar. Substituting $M_{H^\pm} = 70 \text{ GeV}$ and $M_h = 125 \text{ GeV}$ to these bounds yields: $m_{22}^2 < -9.8 \cdot 10^3 \text{ GeV}^2$ or $m_{22}^2 \gtrsim 1.8 \cdot 10^5 \text{ GeV}^2$. Taking into account the bound (2) we are left with the only option:

$$m_{22}^2 < -9.8 \cdot 10^3 \text{ GeV}^2. \quad (5)$$

The conditions (4) can be translated into conditions for the hH^+H^- coupling λ_3 with use of the expression for the mass of the charged scalar: $M_{H^\pm}^2 = \frac{1}{2}(\lambda_3 v^2 - m_{22}^2)$. This gives the following condition:

$$\lambda_3 < 0. \quad (6)$$

4 Results

In this section we present the regions in the parameter space allowed by the constraints (Sec.2.2) and the condition $R_{\gamma\gamma} > 1$. Points with $R_{\gamma\gamma} < 1$ are displayed in dark green (dark gray) and with $R_{\gamma\gamma} > 1$ in light green (light gray).

In Fig. 2 the regions of masses allowed in the IDM by the constraints for the narrow m_{22}^2 range are presented.

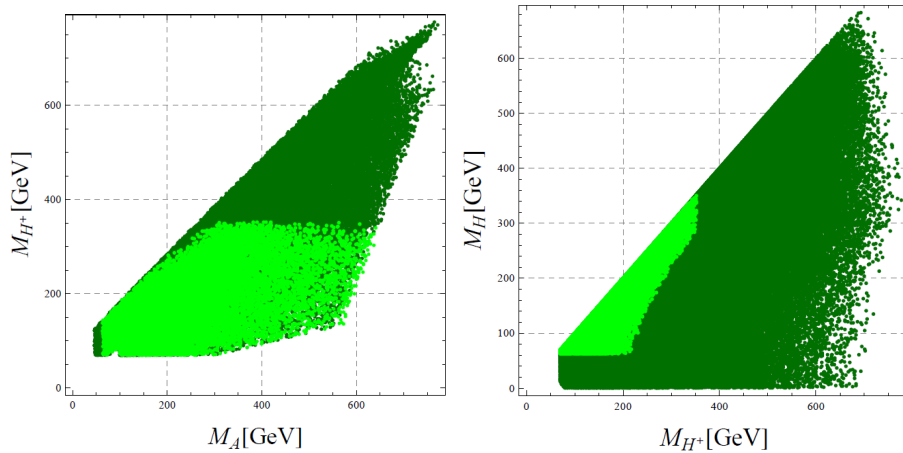


Figure 2: Regions in the (M_A, M_{H^\pm}) (left panel) and (M_{H^\pm}, M_H) (right panel) planes allowed by the constraints for $-25 \cdot 10^4 \text{ GeV}^2 \leq m_{22}^2 \leq 9 \cdot 10^4 \text{ GeV}^2$. Points with $R_{\gamma\gamma} < 1$ ($R_{\gamma\gamma} > 1$) are displayed in dark green/gray (light green/light gray).

²If the contributions from light quarks are neglected, \mathcal{M}^{SM} is real, but we treat it as a complex number, to keep the reasoning general.

We distinguish the regions where the enhancement in the $h \rightarrow \gamma\gamma$ channel occurs. We have found that the $R_{\gamma\gamma}$ enhancement is only possible when $M_H > M_h/2$ and $M_A > M_h/2$. It means that the partial widths of invisible decays increase the total width of the Higgs boson so much that the enhancement with respect to the SM case is impossible (in agreement with results of Ref. [6]).³

The signal in the $h \rightarrow \gamma\gamma$ channel can be enhanced up to almost 3.4 times, which can be inferred from Fig. 3, where the dependence of $R_{\gamma\gamma}$ on M_H and M_{H^\pm} is presented.

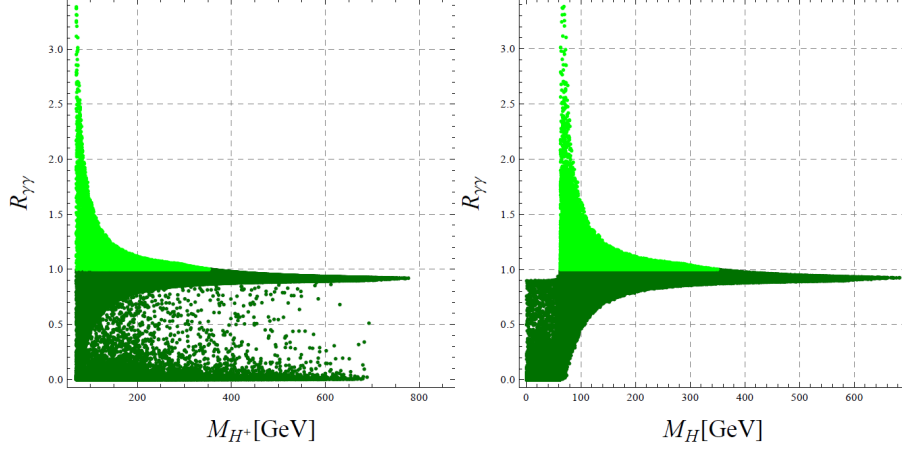


Figure 3: Values of $R_{\gamma\gamma}$ allowed by the constraints for $-25 \cdot 10^4 \text{ GeV}^2 \leq m_{22}^2 \leq 9 \cdot 10^4 \text{ GeV}^2$ as a function of masses: M_{H^\pm} (left panel) and M_H (right panel). Points with $R_{\gamma\gamma} < 1$ ($R_{\gamma\gamma} > 1$) are displayed in dark green/gray (light green/gray).

Fig. 2 and 3 seem to suggest that $R_{\gamma\gamma} > 1$ is only possible for $M_{H^\pm} \lesssim 350 \text{ GeV}$ (compare with the bound $M_{H^\pm} \lesssim 200 \text{ GeV}$ from [6]). However, it is not the case. If we allow for wider m_{22}^2 range, then we get larger M_{H^\pm} for which $R_{\gamma\gamma} > 1$.⁴ This fact is illustrated in the left panel of Fig. 4. In this figure the result of the scan with wider

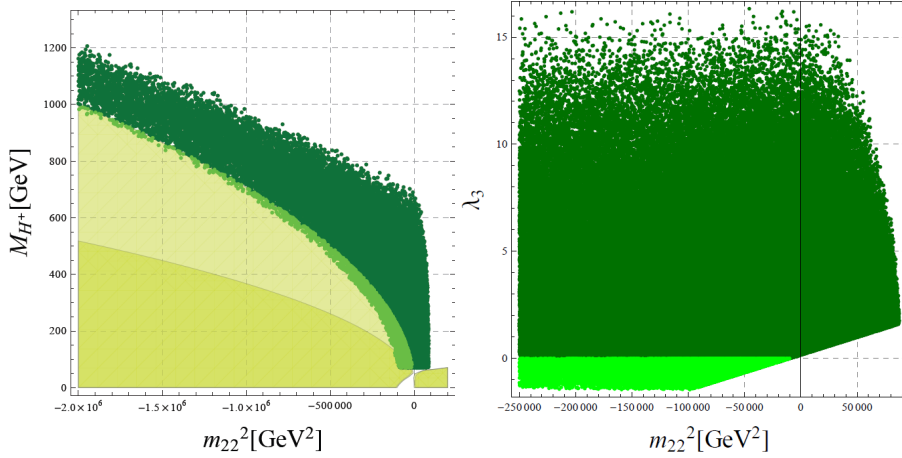


Figure 4: Left panel: region in the (m_{22}^2, M_{H^\pm}) plane where $\tilde{R}_{\gamma\gamma} > 1$ ($\tilde{R}_{\gamma\gamma} > 1.3$) displayed as light shaded (dark shaded) together with the region allowed by the constraints for $-2 \cdot 10^6 \text{ GeV}^2 \leq m_{22}^2 \leq 9 \cdot 10^4 \text{ GeV}^2$, points with $R_{\gamma\gamma} < 1$ ($R_{\gamma\gamma} > 1$) are displayed in dark green/gray (light green/gray). Right panel: region allowed by the constraints for $-25 \cdot 10^4 \text{ GeV}^2 \leq m_{22}^2 \leq 9 \cdot 10^4 \text{ GeV}^2$ in the (m_{22}^2, λ_3) plane. Points with $R_{\gamma\gamma} < 1$ ($R_{\gamma\gamma} > 1$) displayed in dark green/gray (light green/gray).

range of m_{22}^2 is presented together with the region fulfilling $\tilde{R}_{\gamma\gamma} > 1$ (light shaded region) and $\tilde{R}_{\gamma\gamma} > 1.3$ (dark shaded region). Here $R_{\gamma\gamma} > 1$ for M_{H^\pm} up to 1 TeV.

It can be seen from Fig. 3 (left panel) that substantial enhancement ($R_{\gamma\gamma} > 1.3$) appears for relatively light charged scalar, $M_{H^\pm} \lesssim 135 \text{ GeV}$. Moreover, $R_{\gamma\gamma} > 1.3$ is only possible in a region which is bounded ($m_{22}^2 \gtrsim -1.3 \cdot 10^5 \text{ GeV}^2$) (see Fig. 4, left panel) and hence this result does not change if we allow for very big negative m_{22}^2 .

Fig. 3 shows that $R_{\gamma\gamma} \geq 1.3$ also the DM particle has to be light: $M_H \lesssim 135 \text{ GeV}$. So we conclude that substantial enhancement is only possible for:

$$62.5 \text{ GeV} < M_H < 135 \text{ GeV}.$$

³Fig. 2 (left panel) differs from Fig. 1 (left panel) of Ref. [6] as in Ref. [6] the DM particle (H) was assumed to be lighter than the Higgs boson ($M_H < 150 \text{ GeV}$), which decreased the size of the allowed region and also constrained the values of m_{22}^2 , which resulted in tighter upper bounds on the masses of H^\pm and A .

⁴In Ref. [6] m_{22}^2 (or $\mu_2^2 = -1/2m_{22}^2$) was limited by setting $M_H < 150 \text{ GeV}$.

This excludes very light and very heavy DM scenarios.

This reasoning is general and will give upper bounds on M_{H^\pm} and M_H if only $R_{\gamma\gamma} > 1$ is confirmed.

From the left panel of Fig. 4 it is also visible that additional region fulfilling $R_{\gamma\gamma} > 1$ would be allowed for M_{H^\pm} smaller than 70 GeV or m_{22}^2 greater than $9 \cdot 10^4 \text{ GeV}^2$. As in Ref. [6] the conditions determining the existence of the Inert vacuum were not taken into account, the upper bound on m_{22}^2 was not present and in principle a region with $R_{\gamma\gamma} > 1$ and $m_{22}^2 > 0$ could have been allowed in that analysis.

In the right panel of Fig. 4 we present the allowed region in the (m_{22}^2, λ_3) plane and confirm the conclusion of Ref. [6] that the enhanced diphoton production rate is possible only for $\lambda_3 < 0$.

Fig. 5 presents the allowed values of $R_{\gamma\gamma}$ as a function of the couplings λ_3 (hH^+H^- coupling, left panel) and λ_2 (right panel). It can be seen once more that $R_{\gamma\gamma} > 1$ for $\lambda_3 < 0$ and as a consequence, since $M_H < M_{H^\pm}$, also $\lambda_{345} < 0$ with quite stringent lower bounds on both of the couplings: $\lambda_3, \lambda_{345} > -1.5$. If $R_{\gamma\gamma} > 1.3$, then λ_3 is further constrained:

$$-1.45 < \lambda_3 < -0.24.$$

On contrary, $R_{\gamma\gamma} > 1$ is possible for all values of λ_2 (right panel of Fig. 5).⁵

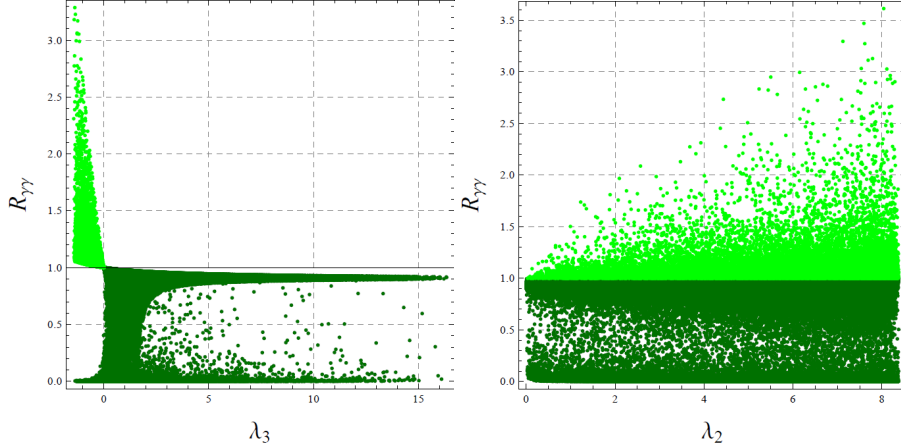


Figure 5: Values of $R_{\gamma\gamma}$ allowed by the constraints for $-25 \cdot 10^4 \text{ GeV}^2 \leq m_{22}^2 \leq 9 \cdot 10^4 \text{ GeV}^2$ as a function of the couplings: λ_3 (left panel), λ_2 (right panel). Points with $R_{\gamma\gamma} < 1$ ($R_{\gamma\gamma} > 1$) displayed in dark green/gray (light green/gray).

5 Summary

We analyzed the diphoton decay channel of the Higgs boson in the IDM. We found that the enhancement in this channel, with respect to the SM, is not possible if the invisible decay channels are open, which confirms the results of Ref. [6]. If the DM particle is heavier than $M_h/2$, then IDM can account for a Higgs boson which has enhanced diphoton rate (with respect to the SM), while its remaining decay channels, in particular $h \rightarrow gg$ and $h \rightarrow Z\gamma$, stay SM-like.

Furthermore, the enhancement is only possible for $m_{22}^2 < -9.8 \cdot 10^3 \text{ GeV}^2$ ($\lambda_3 < 0$) and maximal $R_{\gamma\gamma}$ value reaches 3.4. Substantial enhancement can be realized only if the charged scalar is light (e.g. $R_{\gamma\gamma} > 1.3$ implies $M_{H^\pm} \lesssim 135 \text{ GeV}$). Then, also $62.4 \text{ GeV} < M_H \lesssim 135 \text{ GeV}$, which excludes the light and heavy DM scenarios.

Acknowledgments

We would like to thank A. Arhrib for discussion and materials.

A Derivation of the solution of $R_{\gamma\gamma} > 1$ for $M_H > M_h/2$

We are to solve the following inequality for $M_h = 125 \text{ GeV}$

$$|\mathcal{M}^{\text{SM}} + \delta\mathcal{M}^{\text{IDM}}|^2 > |\mathcal{M}^{\text{SM}}|^2, \quad (7)$$

while \mathcal{M}^{SM} is fixed. Let us use the following definitions: $a = \text{Re}\mathcal{M}^{\text{SM}}$, $b = \text{Im}\mathcal{M}^{\text{SM}}$ and $c = \delta\mathcal{M}^{\text{IDM}} = \frac{2M_{H^\pm}^2 + m_{22}^2}{2M_{H^\pm}^2} A_0(\tau)$, where $\tau = \frac{4M_{H^\pm}^2}{M_h^2}$, $\tau > 1$. Parameter $c \in \mathbb{R}$, because $f\left(\frac{4M_{H^\pm}^2}{M_h^2}\right) = \arcsin^2\left(\frac{M_h}{2M_H}\right)$ for $M_H > M_h/2$.

Hence the inequality (7) can be written as: $|a + ib + c|^2 > |a + ib|^2$ and is equivalent to $c(c + 2a) > 0$.

There are two possibilities: $c > 0$ and $c + 2a > 0$ or $c < 0$ and $c + 2a < 0$. One can compute that $a \approx -6.53 < 0$ so the two cases reduce to: $c > -2a$ or $c < 0$.

⁵It does not agree with the observation of Ref. [5] which stated that $R_{\gamma\gamma} > 1$ for $-\lambda_3 \gg 1$ and only for big values of λ_2 .

$c > -2a \iff \frac{2M_{H^\pm}^2 + m_{22}^2}{2M_{H^\pm}^2} A_0(\tau) > -2a$. $A_0(\tau) = -\tau + \tau^2 \arcsin^2(1/\tau)$, so $A_0(\tau) > 0$ for $\tau > 1$. Therefore we have:

$$m_{22}^2 > \frac{aM_h^2}{1 - \left(\frac{2M_{H^\pm}}{M_h}\right)^2 \arcsin^2\left(\frac{M_h}{2M_{H^\pm}}\right)} - 2M_{H^\pm}^2.$$

$c > 0 \iff 2M_{H^\pm}^2 + m_{22}^2 > 0$ and $A_0(\tau) < 0$ or $2M_{H^\pm}^2 + m_{22}^2 < 0$ and $A_0(\tau) > 0$. As $A_0(\tau) > 0$, the first option is excluded and the other reduces to $m_{22}^2 < -2M_{H^\pm}^2$.

Finally, there are two regions where enhancement in the $h \rightarrow \gamma\gamma$ channel is possible:

$$m_{22}^2 < -2M_{H^\pm}^2 \quad \text{or} \quad m_{22}^2 > \frac{aM_h^2}{1 - \left(\frac{2M_{H^\pm}}{M_h}\right)^2 \arcsin^2\left(\frac{M_h}{2M_{H^\pm}}\right)} - 2M_{H^\pm}^2.$$

B Decay widths of the Higgs boson

Below we summarize the decay widths of the Higgs boson following [24–27].

1. $h \rightarrow q\bar{q}$

$$\Gamma(h \rightarrow q\bar{q}) = \frac{3G_F}{4\sqrt{2}\pi} M_h \bar{m}_q^2(M_h) \left\{ 1 + 5.67 \frac{\bar{\alpha}_s(M_h)}{\pi} + \left[37.51 - 1.36N_f - \frac{2}{3} \log \frac{M_h^2}{m_t^2} + \left(\frac{1}{3} \log \frac{\bar{m}_q^2(M_h)}{M_h^2} \right)^2 \right] \frac{\bar{\alpha}_s^2(M_h)}{\pi^2} \right\}.$$

$N_f = 5$ is the number of active light quark flavors. The running quark mass defined at the scale M_h [26]:

$$\bar{m}_q(M_h) = \bar{m}_q(m_q) \left(\frac{\bar{\alpha}_s(M_h)}{\bar{\alpha}_s(m_q)} \right)^{12/(33-2N_f)} \frac{1 + c_{1q}\bar{\alpha}_s(M_h)/\pi + c_{2q}\bar{\alpha}_s^2(M_h)/\pi^2}{1 + c_{1q}\bar{\alpha}_s(m_q)/\pi + c_{2q}\bar{\alpha}_s^2(m_q)/\pi^2},$$

where for the bottom quark $c_{1b} = 1.17$, $c_{2b} = 1.50$ and for the charm quark $c_{1c} = 1.01$, $c_{2c} = 1.39$. The running strong coupling constant is approximated at the one loop level (for energy scales around M_h , where the number of active light quarks can be taken constant) [27]:

$$\bar{\alpha}_s(M_h) = \frac{\bar{\alpha}_s(M_Z)}{1 + \frac{33-2N_f}{12\pi} \bar{\alpha}_s(M_Z) \log \frac{M_h^2}{M_Z^2}}.$$

The values of quark masses and values of the strong coupling are taken from PDG [27]: $\bar{m}_b(m_b) = 4.18$ GeV, $\bar{m}_c(m_c) = 1.273$ GeV, $\bar{\alpha}_s(M_Z) = 0.118$, $\bar{\alpha}_s(m_b) = 0.223$, $\bar{\alpha}_s(m_c) = 0.38$.

2. $h \rightarrow \tau^+\tau^-$

$$\Gamma(h \rightarrow \tau^+\tau^-) = \frac{G_F N_c}{4\sqrt{2}\pi} M_h m_\tau^2 \left(1 - \frac{4m_\tau^2}{M_h^2} \right)^{3/2}.$$

3. $h \rightarrow VV^*$

$$\Gamma(h \rightarrow VV^*) = \frac{3G_F^2}{16\pi^3} M_V^4 M_h \delta_V R_T(x),$$

where $\delta_W = 1$, $\delta_Z = \frac{7}{12} - \frac{10}{9} \sin^2 \theta_W + \frac{40}{9} \sin^4 \theta_W$,

$$R_T(x) = \frac{3(1-8x+20x^2)}{\sqrt{4x-1}} \arccos\left(\frac{3x-1}{2x^{3/2}}\right) - \frac{1-x}{2x} (2-13x+47x^2) - \frac{3}{2} (1-6x+4x^2) \log x$$

and $x = \frac{M_V^2}{M_h^2}$.

4. $h \rightarrow Z\gamma$

$$\Gamma(h \rightarrow Z\gamma) = \frac{G_F^2 \alpha}{64\pi^4} M_W^2 M_h^3 \left(1 - \frac{M_Z^2}{M_h^2} \right)^3 \left| 2 \frac{1 - \frac{8}{3} \sin^2 \theta_W}{\cos \theta_W} A_{1/2}^h \left(\frac{4m_t^2}{M_h^2}, \frac{4m_t^2}{M_Z^2} \right) + A_1^h \left(\frac{4M_W^2}{M_h^2}, \frac{4M_W^2}{M_Z^2} \right) \right|^2,$$

where:

$$A_{1/2}^h(\tau, \lambda) = I_1(\tau, \lambda) - I_2(\tau, \lambda),$$

$$A_1^h(\tau, \lambda) = \cos \theta_W \left\{ 4 \left(3 - \frac{\sin^2 \theta_W}{\cos^2 \theta_W} \right) I_2(\tau, \lambda) + \left[\left(1 + \frac{2}{\tau} \right) \frac{\sin^2 \theta_W}{\cos^2 \theta_W} - \left(5 + \frac{2}{\tau} \right) \right] I_1(\tau, \lambda) \right\},$$

$$I_1(\tau, \lambda) = \frac{\tau\lambda}{2(\tau-\lambda)} + \frac{\tau^2\lambda^2}{2(\tau-\lambda)^2} [f(\tau) - f(\lambda)] + \frac{\tau^2\lambda}{(\tau-\lambda)^2} [g(\tau^{-1}) - g(\lambda^{-1})],$$

$$I_2(\tau, \lambda) = -\frac{\tau\lambda}{2(\tau-\lambda)} [f(\tau) - f(\lambda)]$$

and

$$g(\lambda) = \begin{cases} \sqrt{\frac{1}{\tau} - 1} \arcsin \sqrt{\tau} & \text{for } \tau \geq 1 \\ \frac{\sqrt{1-\frac{1}{\tau}}}{2} \log \frac{1+\sqrt{1-\frac{1}{\tau}}}{1-\sqrt{1-\frac{1}{\tau}}} & \text{for } \tau < 1. \end{cases}$$

In IDM there is no coupling of H^+H^- to the Z boson, so there is no contribution from the charged scalar loop.

5. $h \rightarrow gg$

$$\Gamma(h \rightarrow gg) = \frac{G_F \alpha_s^2 M_h^3}{36\sqrt{2}\pi^3} \left| \frac{3}{4} A_{1/2} \left(\frac{4m_t^2}{M_h^2} \right) \right|^2.$$

6. $h \rightarrow \varphi\varphi$

$$\Gamma(h \rightarrow \varphi\varphi) = \frac{G_F}{16\sqrt{2}\pi} \frac{M_Z^4}{M_h} \lambda_{h\varphi\varphi}^2 \sqrt{1 - 4 \frac{M_\varphi^2}{M_h^2}},$$

where $\lambda_{hHH} = \lambda_{345}$ and $\lambda_{hAA} = \lambda_{345}^-$.

References

- [1] ATLAS Collaboration, G. Aad *et al.*, Phys.Lett. **B716**, 1 (2012), arXiv:1207.7214.
- [2] CMS Collaboration, S. Chatrchyan *et al.*, Phys.Lett. **B716**, 30 (2012), arXiv:1207.7235.
- [3] ATLAS Collaboration, G. Aad *et al.*, ATLAS NOTE **ATLAS-CONF-2012-168**.
- [4] Q.-H. Cao, E. Ma, and G. Rajasekaran, Phys.Rev. **D76**, 095011 (2007), arXiv:0708.2939.
- [5] P. Posch, Phys.Lett. **B696**, 447 (2011), arXiv:1001.1759.
- [6] A. Arhrib, R. Benbrik, and N. Gaur, Phys.Rev. **D85**, 095021 (2012), arXiv:1201.2644.
- [7] J. Chang, K. Cheung, P.-Y. Tseng, and T.-C. Yuan, Int.J.Mod.Phys. **A27**, 1230030 (2012), arXiv:1211.6823.
- [8] N. G. Deshpande and E. Ma, Phys.Rev. **D18**, 2574 (1978).
- [9] R. Barbieri, L. J. Hall, and V. S. Rychkov, Phys.Rev. **D74**, 015007 (2006), arXiv:hep-ph/0603188.
- [10] I. Ginzburg, K. Kanishev, M. Krawczyk, and D. Sokolowska, Phys.Rev. **D82**, 123533 (2010), arXiv:1009.4593.
- [11] I. F. Ginzburg and M. Krawczyk, Phys.Rev. **D72**, 115013 (2005), arXiv:hep-ph/0408011.
- [12] G. C. Branco, L. Lavoura, and J. P. Silva, *CP Violation* (Oxford University Press, 1999).
- [13] B. Swiezewska, (2012), arXiv:1209.5725.
- [14] S. Kanemura, T. Kubota, and E. Takasugi, Phys.Lett. **B313**, 155 (1993), arXiv:hep-ph/9303263.
- [15] A. G. Akeroyd, A. Arhrib, and E.-M. Naimi, Phys.Lett. **B490**, 119 (2000), arXiv:hep-ph/0006035.
- [16] B. Gorczyca, Unitarity constraints for the Inert Doublet Model (in Polish), Master Thesis at the University of Warsaw, 2011.
- [17] E. M. Dolle and S. Su, Phys.Rev. **D80**, 055012 (2009), arXiv:0906.1609.
- [18] D. Sokolowska, (2011), arXiv:1107.1991.
- [19] L. Lopez Honorez, E. Nezri, J. F. Oliver, and M. H. Tytgat, JCAP **0702**, 028 (2007), arXiv:hep-ph/0612275.
- [20] L. Lopez Honorez, (2007), arXiv:0706.0186.
- [21] Particle Data Group, K. Nakamura *et al.*, J.Phys.G **G37**, 075021 (2010).
- [22] E. Lundstrom, M. Gustafsson, and J. Edsjo, Phys.Rev. **D79**, 035013 (2009), arXiv:0810.3924.
- [23] M. Gustafsson, PoS **CHARGED2010**, 030 (2010), arXiv:1106.1719.
- [24] A. Djouadi, Phys.Rept. **459**, 1 (2008), arXiv:hep-ph/0503173.
- [25] A. Djouadi, Phys.Rept. **457**, 1 (2008), arXiv:hep-ph/0503172.
- [26] A. Djouadi, J. Kalinowski, and P. Zerwas, Z.Phys. **C70**, 435 (1996), arXiv:hep-ph/9511342.
- [27] Particle Data Group, J. Beringer *et al.*, Phys. Rev. D **86**, 010001 (2012).
- [28] M. Spira, Fortsch.Phys. **46**, 203 (1998), arXiv:hep-ph/9705337.